Mini Review

BIOMEDICAL Journal of Scientific & Technical Research

ISSN: 2574 -1241

DOI: 10.26717/BJSTR.2026.67.010421

A Minireview on Engineering Closed Pores in Hard Carbon Anodes for Sodium-Ion Batteries

Wenlan Fan[1], Guiyun Yi[1]* and Jie Wang[2]

[1]*College of Chemistry and Chemical Engineering, Henan Polytechnic University, Jiaozuo 454003, China*

[2]*HuaXia Besince environmental technology CO. LTD, China*

***Corresponding author:** Guiyun Yi, College of Chemistry and Chemical Engineering, Henan Polytechnic University, Jiaozuo 454003, China

ARTICLE INFO

Received: September 09, 2026

Published: October 01, 2026

Citation: Wenlan Fan, Guiyun Yi and Jie Wang. A Minireview on Engineering Closed Pores in Hard Carbon Anodes for Sodium-Ion Batteries. Biomed J Sci & Tech Res 67(1)-2026. BJSTR. MS.ID.010421.

ABSTRACT

The low-voltage plateau capacity of hard carbon (HC) anodes in sodium-ion batteries (SIBs) is a critical determinant of the battery's energy density, with its sodium storage mechanism heavily reliant on the closed pore structure within the material. However, due to their inaccessibility to external environments, conventional characterization techniques face challenges in directly probing internal structural information, resulting in ongoing academic debates regarding the "pore filling" and "quasi-metallic Na cluster deposition" mechanisms for sodium storage. This has emerged as a significant barrier to achieving rational design of HC materials. This review focuses on closed pores and provides a comprehensive examination of the evolving understanding of the sodium storage mechanism, transitioning from indirect deduction to direct observation through advanced multimodal in situ characterization techniques. It establishes that the dominant viewpoint posits sodium storage within closed pores occurs primarily in the form of quasi-metallic clusters. The study synthesizes insights into the synergetic regulation of closed pore size, pore volume, and interlayer spacing on plateau capacity, offering rational design strategies at three distinct levels: molecular engineering, carbonization process optimization, and microstructural synergy. Additionally, the research explores future directions, including multi-scale characterization approaches, data-driven modeling, and interface coupling mechanisms, which hold promise for advancing the development of high-performance hard carbon anodes.

Keywords: Sodium-Ion Battery; Hard Carbon Anodes; Closed Pores; Quasi-Metallic Sodium; In Situ Characterization

Abbreviations: HC: Hard Carbon; SIBs: Sodium-Ion Batteries; EPR: Electron Paramagnetic Resonance; PDF: Pair Distribution Function; SSNMR: Solid-State Nuclear Magnetic Resonance; SANS: Small-Angle Neutron Scattering; WANS: Wide-Angle Neutron Scattering; ICE: Initial Coulombic Efficiency; SAXS: Small-Angle X-Ray Scattering; SEI: Solid-Electrolyte Interphase

Introduction

Sodium-ion batteries have demonstrated substantial industrialization potential in specific applications such as large-scale energy storage systems and low-speed transportation due to their inherent advantages including abundant sodium resource availability (~2.64%) [1], wide geographic distribution, and minimal geographical constraints. Among various anode materials, hard carbon currently stands as the sole system achieving industrial application, with companies like Kureha and China National Sodium Energy Technology leading the establishment of a comprehensive industrial chain [2,3]. However, the fundamental challenge in rationalizing HC design persists due to insufficient understanding of the sodium storage mechanism within the low-voltage plateau region, which remains the primary source of their elevated capacity. The sodium insertion process in HC exhibits two distinct regions: a high-potential region (>0.1 V) and a low-voltage plateau region (<0.1 V). The sloped region is generally attributed to sodium ion adsorption at carbon layer defects and open pore surfaces, while the plateau region displays a flat potential characteristic closely aligned with the deposition potential of metallic sodium. Extensive studies have consistently shown that the high specific capacity of hard carbon is predominantly contributed by the low-voltage plateau region, with its sodium storage mechanism intricately linked to the unique closed pores within the material [4-6].

DOI: 10.26717/BJSTR.2026.67.010421

However, a lack of consensus exists in academia regarding whether the sodium storage mechanism in this region follows a pore-filling or quasi-metallic sodium cluster deposition pathway. Furthermore, the isolation of closed pores from external environments complicates direct structural analysis using conventional gas adsorption and diffraction techniques, leaving researchers reliant on indirect inference through electrochemical signals. This lack of clarity concerning the structure-activity relationship remains a pivotal obstacle hindering advancements in high-performance hard carbon anodes. In recent years, advanced multimodal in situ characterization techniques (in situ transmission electron microscopy, small-angle X-ray scattering, and neutron scattering) have emerged to overcome the limitations of traditional characterization methods. These cutting-edge tools now enable real-time observation of closed pore evolution and sodium occupancy at atomic and nanoscale resolutions [7,8]. However, despite their potential, these techniques still face significant challenges. For instance, achieving a balance between spatial resolution and compatibility with realistic battery environments remains problematic. Additionally, the use of electron beams or probes in such techniques often disturbs sample structures, while idealized model systems derived from laboratory conditions may not fully extrapolate to practical materials.

As a result, there is an urgent need to systematically unravel the comprehensive relationship chain governing closed pore formation, evolution, and sodium storage. Therefore, this article takes closed pores as the core theme, systematically reviews the current research progress from three dimensions (cognitive evolution and characterization technology innovation of sodium storage mechanism, formation and structure-activity regulation of closed pores, and rational design strategies). Finally, key challenges and future directions are discussed, and some guidance for the design of carbon materials are also provided.

Cognitive Evolution of Sodium Storage Mechanism in Plateau Regions

Sodium Storage Mechanism

In the study of hard carbon anodes in sodium ion batteries, the electrochemical behavior within the low-voltage plateau region has been identified as a critical factor influencing energy density [9]. This understanding begins with a clear distinction between intercalation and filling processes and is progressively refined through iterative advancements in characterization techniques. Over time, this cognitive framework evolves into a more sophisticated multivariate model dependent on precursor materials.

Evolution of Sodium Storage Mechanism in the Plateau Region: In 2000, Stevens and Dahn first proposed an "intercalation-filling" model based on glucose pyrolysis of hard carbon, combining wide-angle and small-angle X-ray scattering to classify the plateau region as the physical filling of sodium within nanopores [10,11]. However, the chemical state of sodium in the pores cannot be directly determined by scattering techniques. In 2012, Cao, et al. [12] challenged this paradigm by proposing that the low-voltage plateau region corresponds to sodium intercalation between graphite-like layers, thereby questioning the pore filling hypothesis. Three years later, Bommier and Ji incorporated electron paramagnetic resonance (EPR) technology to demonstrate a linear correlation between ramp capacity and carbon defects, as revealed through spin state analysis. This breakthrough established a three-stage mechanism involving defect adsorption, intercalation, and pore surface adsorption [13]. In 2016, two pivotal experiments redirected academic research toward understanding closed pore filling mechanisms. Zhang, et al. [14] discovered that ultra-high temperature carbonized PAN fibers exhibited only a plateau region without a slope region during charge and discharge cycling, with no observable shifts in XRD interlayer spacing peaks throughout the process.

If intercalation were a universal mechanism within the plateau region, detectable responses in interlayer spacing would be expected. Concurrently, Li, et al. [15] confirmed that the Na1s binding energy reversibly approached the characteristic value of metallic sodium during the plateau region, while the carbon interlayer spacing remained constant. These findings established the pore filling mechanism, and identified closed pores as the true active sites. In 2020, Au, et al. [16] conducted ex situ 23Na solid-state nuclear magnetic resonance (ssNMR) and pair distribution function (PDF) analyses, observing a continuous chemical shift of sodium within closed pores from approximately 600 ppm to about 1100 ppm as the filling depth increased. This indicated that sodium undergoes a gradual metallization process in the pores rather than a sudden phase transition from ionic to metallic state. This discovery provided a direct spectroscopic criterion for determining the chemical state of sodium stored within closed pores. Subsequently, reviews [17,18] and in situ nuclear magnetic resonance studies by Wang, et al. [19] further confirmed that quasi-metallic sodium is the primary sodium storage form in the low-voltage plateau region (Figure 1b).

The current academic consensus on precursor-dependent hybrid models posits that hard carbon with a high degree of graphitization and low closed porosity predominantly follows intercalation mechanisms, while hard carbon with a high closed pore rate and low graphitization degree is dominated by pore filling [20,21]. Eren, et al. [22] proposed a three-stage adsorption-accumulation-filling model for sodium storage in hard carbon, subdividing the plateau region into two sub-stages: the initial formation of quasi-metallic monolayers and the subsequent filling of multilayer clusters (Figure 1d). In 2026, Umemoto, et al. [23] quantitatively elucidated the sequential mechanism of surface adsorption, intercalation into interlayers, and nanopore filling for commercial hard carbon using operando small-angle neutron scattering (SANS) and wide-angle neutron scattering (WANS) techniques combined (Figure 1e).

DOI: 10.26717/BJSTR.2026.67.010421

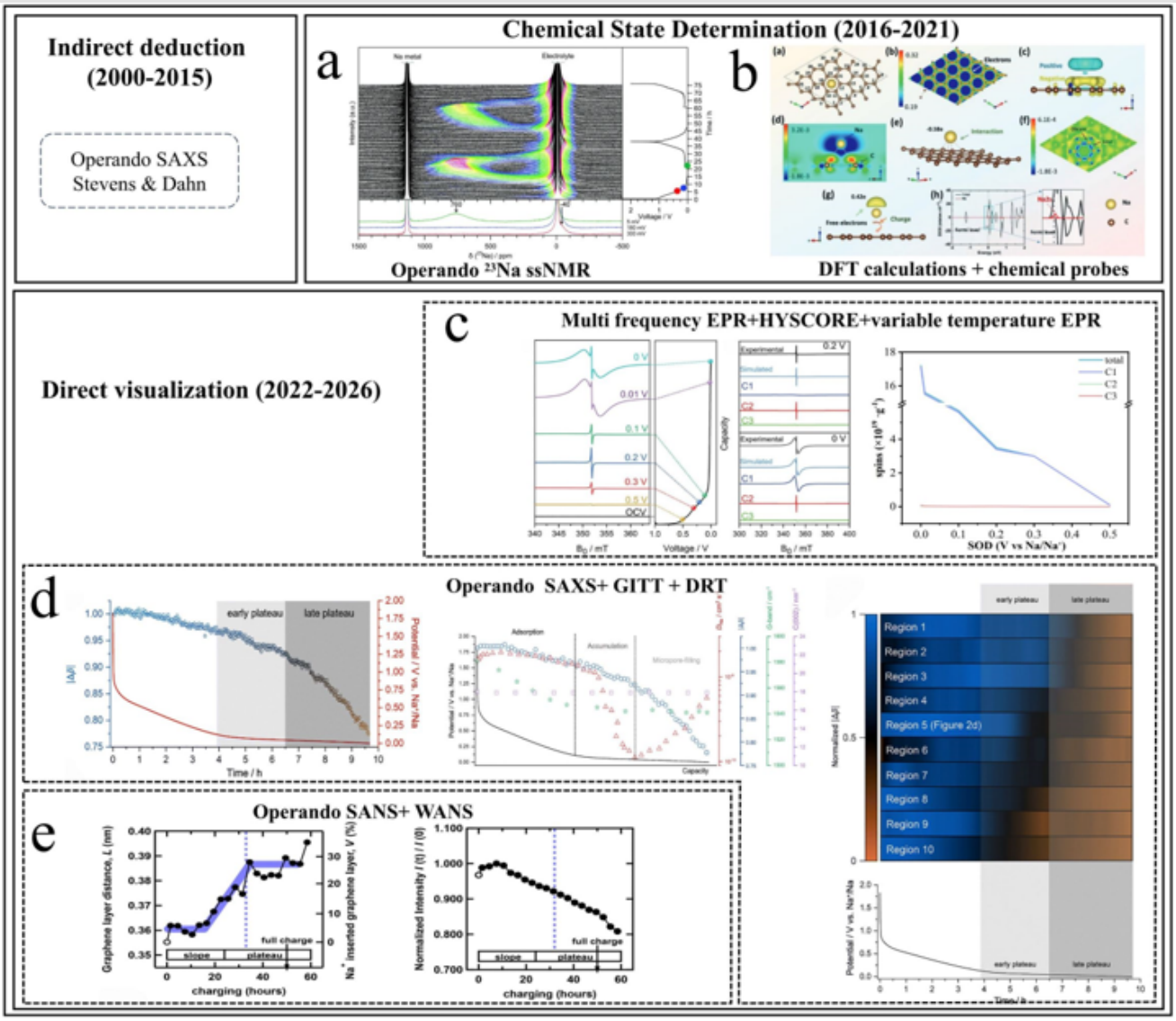

Figure 1: Timeline of multimodal in situ characterization techniques and the cognitive evolution of sodium storage mechanisms in closed pores.

a) Operando ²³Na ssNMR spectra recorded during discharge, revealing the gradual positive shift of Na resonance from the sloping to the plateau region and indicating progressive metallization of sodium [30];

b) DFT-calculated charge density difference, Bader charge transfer, and density of states of Na adsorbed on graphene, confirming the formation of quasi-ionic bonds and the presence of free electrons at the Fermi level [19];

c) Multi-frequency EPR spectra deconvoluted into three components (C1, C2, and C3), identifying Na^+ intercalation, quasi-metallic Na clusters, and Na^+-solvent co-intercalation, respectively, with the corresponding spin counts as a function of discharge depth [36];

d) Operando SAXS analysis showing the variation of relative electron density contrast ($\Delta\bar{\rho}$) across the plateau region, together with the three-stage "adsorption-accumulation-filling" model comprising the slope, early-plateau, and late-plateau stages [22];

e) Simultaneous operando SANS and WANS measurements revealing the sequential Na storage process: initial surface adsorption, subsequent intercalation into graphene layers, and final nanopore filling [23].

DOI: 10.26717/BJSTR.2026.67.010421

Innovation in Characterization Technology: The breakthrough in characterization technology often drives the innovation of sodium storage cognition. Small-angle X-ray scattering (SAXS) defines the physical boundaries of the problem, EPR introduces independent information in the spin dimension, and solid-state nuclear magnetic resonance provides a direct criterion for chemical states. The following sections elaborate on the key characterization methods for constructing the closed pore sodium storage cognitive system layer by layer, based on the chronological development of these technologies. The introduction of SAXS technology has enabled the first-time achievement of intuitive and quantitative observations of closed pores, thereby revealing the positive correlation between closed pore volume and plateau capacity. This advancement has successfully transformed the ambiguous electrochemical phenomenon into a well-defined physical filling process within the pores [24]. Subsequently, helium pycnometry is introduced as a complementary approach to indirectly estimate closed pore volume by comparing the difference between true density and apparent density [25]. Through the integration of multiple methods, quantitative insights into the evolution of electron density during the pore-filling process [26] and spatially resolved imaging of electrode-scale pore filling were obtained [27].

However, SAXS fitting relies on an idealized pore model, which deviates from vacuum pores and complicates the identification of fully saturated filled pores [7]. The introduction of 23Na solid-state nuclear magnetic resonance (ssNMR) has fundamentally elucidated the steady-state chemical nature of sodium [28,29]. In 2016, Stratford, et al. [30] firstly employed in situ 23Na ssNMR to observe the reversible appearance of peaks with partial metallic characteristics within the low-voltage plateau region (Figure 1a). This observation strongly suggests the presence of closed pores containing steady-state quasi-metallic sodium [19]. Subsequently, Gotoh [31] identified that quasi-metallic sodium clusters are located at ppm ranging from 700 to 1100, while the Knight shift for bulk metallic sodium is approximately 1130 ppm. These findings have provided a clear spectroscopic resolution to the debate regarding the chemical state of sodium in the plateau region. In 2025, Gabrijelčič, et al. [32] advanced the field by employing time-resolved 23Na ssNMR, confirming that the adsorption of ion states on pore walls and quasi-metallic clustering within pore cavities are two distinct processes characterized by completely different relaxation times. The study quantitatively presented the fluctuation of these processes with discharge depth on a time-resolved chemical shift map, offering deeper insights into the dynamic behavior of sodium during battery operation.

The Operando Raman study published by Weaving, et al. [33] in 2020 showed that the reversible redshift of the G band in the slope region is due to the charge transfer from the embedded sodium to the π* antibonding orbitals in the carbon layer, weakening the C-C bond. Upon entering the plateau region, the displacement of the G band ceases, signifying that intercalation reaches saturation before plateau formation. The disappearance of the D band in the deep discharge state is not indicative of structural ordering but rather reflects the filling of the conduction band empty states required for the D-band double resonance process, driven by an upward shift in the Fermi level [34]. This suggests that changes in the D band correspond to variations in electronic occupancy rather than structural rearrangement. Yun, et al. [35] provided XPS evidence supporting the following findings. The Na1s binding energy of graphitized carbon nanosheets reversibly shifts toward lower values within the low-voltage plateau region (~0.1 V), approaching the characteristic value associated with metallic sodium. Raman and XPS together offer a synergistic view of sodium's electronic trajectory as it transitions from an ionic to a quasi-metallic state, observed through phonon and core energy windows. XANES, EPR, and electron tomography form a multi-dimensional verification framework that bridges electronic states and spatial morphology, advancing our understanding of closed-pore sodium storage from indirect deduction to direct visualization.

XANES can distinguish oxidation states and coordination environments by detecting the energy shift of the sodium K-edge. Multi-frequency EPR provides independent paramagnetic evidence for multi-step electronic state transitions of sodium (Figure 1c), corresponding to interlayer-embedded sodium (wide signal ~12 mT), quasi-metal clusters (narrow signal ~0.55 mT), and solvent-co-embedded species (extremely narrow signal) [36]. In 2025, two notable advancements have push closed-pore sodium storage toward direct visualization. Sun, et al. [37] utilized HAADF-STEM electron tomography to reconstruct the spatial distribution of closed pores in a sub-volume of 23.9 × 29.6 × 33.1 nm3 and employed low-dose aberration-corrected TEM to directly capture the deposition morphology of sodium clusters within closed pores. In the same year, Zhang, et al. [34] redefined the decisive role of solvation structure in closed-pore sodium storage through multi-modal in situ characterization. However, these three characterization techniques emphasize different aspects: spatial resolution, statistical representativeness, and in situ testing capabilities. This inherent trade-off makes it challenging for any single method to independently construct a complete physical image of closed-pore sodium storage. As such, multi-dimensional complementarity emerges as an inevitable choice for unraveling the mechanism behind sodium storage.

Formation Mechanism and Structure-Activity Regulation of Closed Pores

Formation and Classification of Closed Pores: Closed pores are structural features formed during the pyrolysis process [32], where interconnected open pores undergo continuous cross-linking, bending, and folding of graphene layers, ultimately becoming isolated from external access (Figure 2a). During the low-temperature pyrolysis stage, chemical bonds within the precursor are cleaved to generate free radicals, releasing volatile products such as H2, CH4, and CO, which result in significant weight loss. Simultaneously, non-carbon substances are

 DOI: 10.26717/BJSTR.2026.67.010421

removed, and initial open pores are formed [38]. Due to the thermosetting cross-linked skeleton of the hard carbon precursor, it does not undergo macroscopic melting during subsequent high-temperature treatment, but mainly grows microcrystals, suppressing the complete collapse of the pore structure [25]. The formation of graphite microcrystals signifies the onset of graphitization, characterized by a reduction in interlayer spacing and an increase in interlayer bonding forces. As temperatures rise further, carbon nanosheets shared between adjacent pores rotate and stack, facilitating the merging of small-sized pores. Concurrently, graphite microcrystals continuously wrap around and shrink open pores, gradually closing them while leaving only a very small entrance, ultimately transforming into closed pores [5,7]. This process involves not only physical pore formation but also chemical bond rearrangement.

The bending of the carbon layer on the pore wall introduces topological defects such as pentagonal and seven-membered rings, imparting unique local curvature and electronic density of states distributions to the closed pore walls. Properly sized closed pores can effectively accommodate sodium clusters, thereby enhancing the sodium storage performance of hard carbon. Additionally, pore walls with a lower degree of graphitization provide active sites for sodium ion adsorption. However, it should be noted that excessively high heat treatment temperatures may lead to complete pore closure, diminishing accessible diffusion channels for sodium ions. Gan, et al. [5] categorized closed pores into three levels based on their accessibility. Quasi-closed pores (0.35-0.5 nm) allow solvent penetration but contribute limited plateau capacity while being prone to SEI film growth, which results in irreversible sodium ion consumption. While, closed pores (<0.35 nm) repel solvents and only permit Na^+ entry, efficiently contributing reversible capacity and improving initial Coulombic efficiency (ICE). Fully closed pores are completely sealed, preventing Na^+ ingress and ceasing capacity contribution (Figure 2b). The 0.35 nm threshold aligns precisely with the size of the solvation shell of Na+, revealing that pore size acts as a selective checkpoint for ion desolvation kinetics [25].

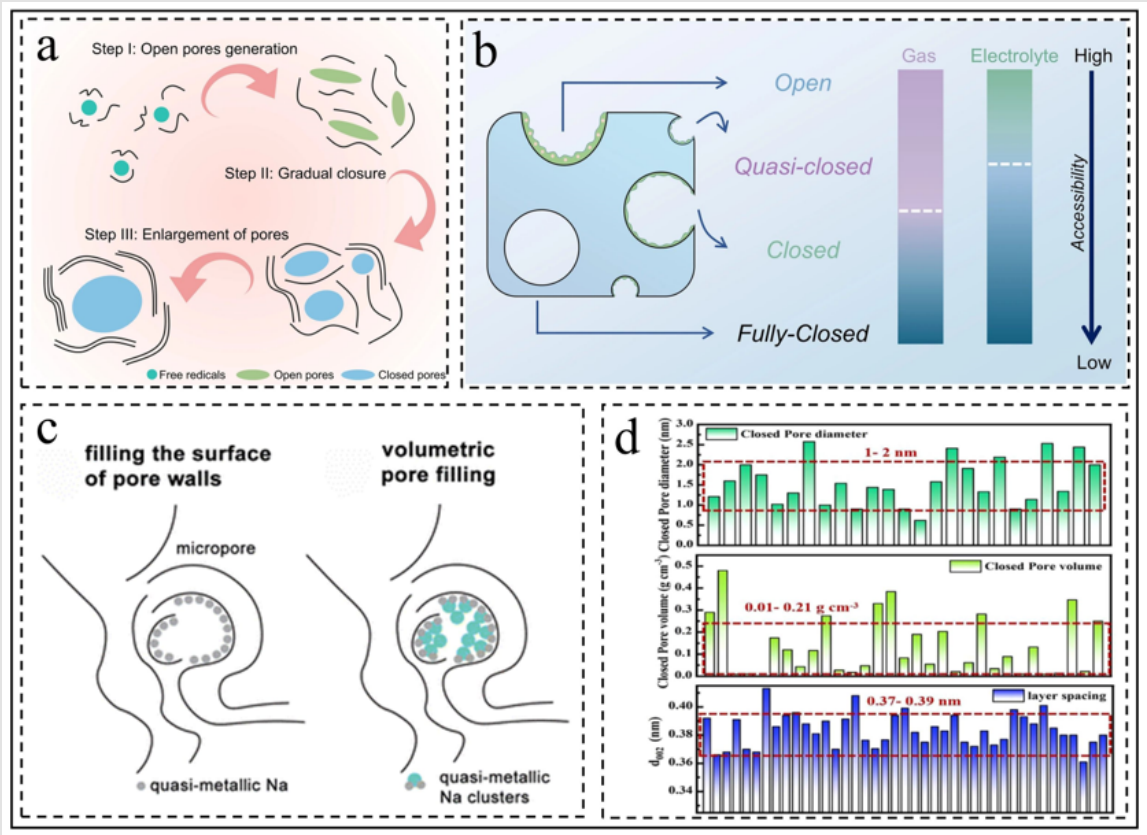

Figure 2:

a) Formation of closed pores [5];
b) Three classifications of closed pores [5];
c) Closed pore sodium storage mechanism [32];
d) Closed pore characteristic parameters [6].

DOI: 10.26717/BJSTR.2026.67.010421

The Synergistic Effect of Closed Pore Size and Pore Volume: At the microdynamic level, multiple independent studies [5,39] have reached a consensus on the two-step mechanism of pore filling: the first stage involves ion monolayer adsorption onto the pore wall, where capacity is proportional to the specific surface area within the pore, and the physical image closely resembles BET monolayer coverage. The second stage entails the adsorbed sodium ions acquiring electrons (Figure 2c), partially shedding their solvation shell, migrating toward the interior of the pore cavity, and aggregating into quasi-metallic sodium clusters, forming a physical image similar to the transition from BET multilayer adsorption to capillary condensation [32]. The critical entrance size for sodium atom nucleation is 0.63 nm, with the minimum critical nucleus containing a single sodium atom; conversely, the maximum pore size that can accommodate mature and stable clusters reaches 1.98 nm, equivalent to six layers of sodium atoms. In summary, whether closed pores can effectively enhance the capacity of hard carbon plateaus depends on the synergistic optimization of pore size and pore volume. Pore size determines the thermodynamic stability of sodium clusters within the pore, while pore volume dictates the theoretical upper limit of total capacity.

Experimental data reveal a clear optimal window for both parameters: the optimal closed-pore size is 1-2 nm, with a corresponding pore volume range of 0.01-0.21 cm3·g-1 and an interlayer spacing of 0.37-0.39 nm [6] (Figure 2d). When the pore size falls below 1 nm, the confined space becomes insufficient to support the nucleation of multi-atomic quasi-metallic sodium clusters, leaving the sodium storage mechanism restricted to monolayer ion adsorption on the pore wall. Conversely, when the pore size exceeds 2 nm, the confinement effect weakens, causing the thermodynamic stability of sodium clusters to shift toward bulk metallic sodium and increasing the risk of irreversible dendritic deposition. Regarding pore volume variation, Gabrijelčič, et al. [32] demonstrated a volcano-shaped relationship between plateau capacity and closed-pore volume using carbonization temperature as a variable. Only single-layer adsorption occurs at 900 °C, while the optimal range is achieved at 1400 °C, quasi-metallic sodium clusters form, and capacity peaks. Beyond 1600 °C, pore merging and rupture lead to a decline in capacity.

Precursor Dependence

The structure-activity relationship of closed pores exhibits significant precursor dependence, with their morphology, chemical activity, and connectivity partially constrained by the precursor molecular skeleton prior to carbonization [40,41]. For instance, biomass precursors naturally possess a hierarchical pore structure and abundant oxygen-containing functional groups. However, their closed pores tend to shrink from the original initial micropores [42,43]. While this pathway utilizes cheap and renewable raw materials, it faces challenges in achieving consistent structural uniformity. Phenolic resin stands out as a notable precursor due to its ability to form highly curved carbon layers through synergistic rearrangement of local chemical bonds during pyrolysis. This process generates a large number of ideal closed pores (<0.4 nm) without the pore-forming agents, which makes it the closest analog to model carbon. Polyacrylonitrile represents the third pathway, undergoing stepwise thermochemical reactions such as cyclization and dehydrogenation to form a dense turbine-layered carbon structure.

The closed pores in this case primarily originate from the voids formed between layers after thermal decomposition of heteroatoms, characterized by higher residual defect concentrations and more complex pore size distributions [14]. These three precursors correspond to distinct closed-pore generation logics, with key parameters such as pore wall chemical activity, pore size geometry, and inter-pore spatial connectivity partially determined during precursor selection [7].

Rational Design Strategy for Closed Pores

Building on the understanding of the structure-activity relationship outlined above, researchers have developed multi-level strategies for closed-pore engineering, spanning precursor molecule design, carbonization process optimization, and collaborative regulation of microstructure parameters. These efforts aim to maximize plateau capacity while balancing considerations of ICE performance and rate performance [5,7,44]. Table 1 provides a comparative analysis of sodium storage performance for representative hard carbon anodes across six strategy categories: cross-linking, pore-forming agents, heteroatom doping, pre-carbonization/oxidation, Flash Joule heating, and chemical vapor deposition (CVD).

 DOI: 10.26717/BJSTR.2026.67.010421

Table 1: Comparison of sodium storage performance of hard carbon anodes under different closed-pore engineering strategies.

Treatment	Precursor	Current Density (mA g^{-1})	Reversible Capacity (mAh g^{-1})	ICE	Ref.
Cross-linking	Corn starch	30	384.9	85.2	[47]
	Switchgrass	100	313.4	84.8	[46]
Pore-forming agents	Bamboo	30	339.2	86.3	[50]
	Elastomer SBS	50	391	77.4	[53]
	Camellia shell	50	340	73	[51]
Heteroatom doping	Resin	25	328	71	[54]
	Resorcinol-formaldehyde resin	50	367.9	76	[44]
	Corn starch	30	341.3	86.9	[55]
	Pitch	20	416.1	89.7	[48]
Pre-carbonization	Mangosteen shell	20	308	81.8	[42]
	Tannin extract	30	360.96	82.08	[61]
Pre-oxidation	Cellulose	20	426.8	74.8	[45]
Flash joule heating	Microcrystalline cellulose	25	377	93.3	[62]
CVD	Resin	10	335	94	[64]

Precursor Molecular Engineering

The precursor molecular structure serves as the foundation for closed pore regulation, encompassing three principal pathways: crosslinking, pore-forming agents, and heteroatom doping. These strategies collectively influence the skeleton construction of the carbon materials, pore cavity formation, and modulation of the carbon layer microenvironment prior to carbonization.

Cross-Linking: The degree of cross-linking in the precursor directly governs the evolution pathway of the pore structure during the carbonization process. Insufficient cross-linking leads to excessive skeleton shrinkage, hindering the formation of closed pores. Conversely, excessive cross-linking impedes the growth of graphite microcrystals. Oxidative pretreatment introduces additional carbonyl and carboxyl crosslinking sites in cellulose, thereby enhancing the closed pore rate and interlayer spacing [45]. Hydrothermal treatment leverages the dissolution and repolymerization effects of subcritical water to reconstruct carbon precursors with uniform cross-linking density [46]. Notably, two independent studies from 2024 achieved precise control over closed pore volume and plateau capacity through starch cross-linking regulation [47] and a phosphorus/oxygen double cross-linking strategy [48], respectively. Among these, the phosphorus/oxygen double cross-linked asphalt-derived hard carbon exhibited a reversible capacity of 416.1 mAh·g-1 and an ICE (inherent crystalline electrolyte) efficiency of 89.7%. Liu, et al. [49] elucidated the chemical-mechanical coupling mechanism of pore closure during carbonization by examining the connectivity, spatial uniformity, and rheological evolution of cross-linked networks from a molecular topology perspective.

Pore Forming Agent: Pore-forming agents not only augment pore volume but also enhance the overall degree of disorder in the material, furnishing a structural basis for the transition from open to closed pores. Based on their chemical properties, these agents can be categorized into three types: gas-phase, inorganic, and organic. Gas-phase pore-forming agents such as CO2, NH3, or water vapor, are incorporated into micropores through carbon gasification reactions during carbonization, followed by pore closure at elevated temperatures. Among these, CO2 activation has demonstrated a preference for increasing the proportion of closed pores [50]. Inorganic template agents like ZnO and KOH are dispersed within the precursor matrix, of which ZnO is subsequently reduced to metallic Zn via carbothermal reduction at temperatures exceeding 907 °C and evaporates, leaving behind uniform cavities [51]. Organic template agents including carbon quantum dots [52] and block copolymers [53] occupy spatial positions during the early stages of carbonization and thermally decompose later, enabling precise control over closed pore size.

Heteroatom Doping: The incorporation of heteroatoms such as phosphorus (P), sulfur (S), and nitrogen (N) into carbon layers not only alters their electronic structure but also significantly influences the formation mechanism of closed pores [54,55]. For instance, Ando, et al. [44] demonstrated that P-doped hard carbon can form sodium clusters with quasi-metallic characteristics even at relatively low carbonization temperatures of 1100 °C. This material exhibits a notably higher plateau capacity compared with the undoped counterparts. The larger covalent radius of phosphorus atoms facilitates an expansion of the local carbon interlayer spacing, thereby substantially reducing the energy barrier for sodium ion migration from the interlayer to the closed pore structure. Additionally, Yadav & Dutta [56]

DOI: 10.26717/BJSTR.2026.67.010421

conducted a comprehensive review on the synergistic regulatory effects of metal single-atom doping on both the electronic structure and closed pore characteristics in hard carbons. Furthermore, heteroatom dual-doping can effectively enhance electrochemical performance.

Pretreatment and Carbonization Process Optimization: The regulation of carbonization process is essentially seeking precise matching between thermodynamic driving force and dynamic path, which constitutes the core step toward attaining optimal closed pores. The following discussion will address this topic from three distinct angles: pre-carbonization and oxidation treatment, temperature rise rate regulation, and microstructure synergy.

Pre Carbonization and Oxidation: Introducing a low-temperature pre-carbonization stage prior to high-temperature carbonization serves to eliminate most volatile substances in advance. This prevents uncontrolled pore structure expansion and rupture that could occur during the intense release phase at higher temperatures. Lan, et al. [42] employed mangosteen shell as a precursor to elucidate the regulatory mechanism of pre-carbonization temperature on biomass thermochemical competitive reactions. Their findings revealed that pre-carbonization at 500 °C promotes the formation of oxygen-containing polycyclic aromatic hydrocarbons, leading to the subsequent development of rich closed pores and enlarged carbon interlayer spacing after high-temperature carbonization. In contrast, pre-carbonization at 400 °C tends to produce open pores, while a temperature of 600 °C results in numerous open pores and micropores. Oxidation treatment plays a crucial role in adjusting the quantity and primary types of defects and functional groups, thereby influencing the activation level and pyrolysis process of the crosslinking system [57].

For precursors with low softening points such as asphalt, oxidation stabilization is a critical step to prevent melting and merging during high-temperature carbonization [58-60]. By integrating oxidation stabilization, low-temperature pre-carbonization, and high-temperature carbonization into a three-step strategy, the cross-linking state, volatile matter release rhythm, and carbon layer rearrangement process can be systematically regulated. This approach ultimately results in a significant improvement in the retention rate of closed pore volume [61].

Heating Rate and New Carbonization Technology: The regulation of heating rates fundamentally represents a dynamic interplay between the kinetics of carbon layer rearrangement and the release of volatile matter. When employing slow heating at 1-5 °C·min-1, this process is found to be highly conducive to the ordered growth of graphite microcrystals while simultaneously promoting the gradual formation of closed pores, ultimately resulting in uniformly sized closed pores. Conversely, rapid heating at 20 °C·min-1 accelerates the release of volatile substances, leading to significant increases in pore volume and a broader distribution of pore sizes. The setting of the final carbonization temperature also needs to be balanced between the plateau capacity and the initial coulombic efficiency (ICE). Typically, temperatures within the range of 1400-1600 °C are identified as the sweet spot for optimizing both closed pore rates and pore size. However, when the carbonization temperature exceeds 1800 °C, there is a marked increase in graphitization, which unfortunately leads to the merging or even collapse of closed pores. This adverse effect hinders the penetration of electrolytes and sodium ions, thereby impairing the overall performance of the material. Recent advancements in carbonization technologies have introduced innovative solutions to address these challenges.

Notably, Flash Joule heating has emerged as a groundbreaking technique [62,63], capable of rapidly heating precursors to temperatures as high as 3000 °C before implementing swift cooling within seconds. This approach effectively suppresses excessive graphitization and prevents the coalescence of closed pores by leveraging an extremely narrow heat treatment window. Complementary to this, chemical vapor deposition has been employed to construct amorphous carbon layers in situ on the surface of hard carbons. This method selectively blocks micropores and transforms them into closed pores, thereby significantly increasing the volume of closed pores, approximately nine times greater than before. Simultaneously, organic free radicals are utilized to repair surface defects, protect carbonyl groups from reduction, and inhibit the formation of the solid-electrolyte interphase (SEI) on the inner walls of pores [64].

Collaborative Regulation of Microstructure: It is imperative to recognize that the practical application of hard carbon anodes should not be myopically focused solely on closed pore volume as a singular metric. Rather, the effective utilization of hard carbon anodes necessitates a holistic optimization strategy that considers and balances three critical factors: the configuration of closed pores, interlayer spacing, and defect concentration [6,65]. The interlayer spacing dictates the smoothness of sodium ion transport channels. A minimum interlayer spacing of approximately 0.37 nm is essential for effective sodium storage, with the optimal range lying between 0.37 nm and 0.39 nm. When the interlayer spacing becomes too narrow (below 0.36 nm), the energy barrier for sodium insertion significantly increases, impairing the efficient transport of sodium ions into the pore despite sufficient closed pore volume. While a controlled concentration of defects facilitates the initial capture and interlayer diffusion of sodium ions, an excessive concentration can lead to irreversible sodium binding and disrupt the orderly growth of graphite microcrystals [13]. Ultimately, closed pores are the core carrier of plateau capacity, but improving the reversible capacity of sodium ions also depends on the synergistic effect of interlayer spacing and defect sites.

Summary and Outlook

In interpreting the sodium storage mechanism within the hard carbon low-voltage plateau region, closed pores serve as the core element. This article takes the development of characterization technology as a clue to sort out the cognitive transition of sodium storage

mechanism from indirect deduction by SAXS to direct visualization by electron tomography imaging. It identifies and summarizes the regulatory principles governing key parameters such as closed pore size, pore volume, and interlayer spacing in relation to plateau capacity. But to achieve the key leap from empirical optimization to rational design, it still relies on breakthroughs in multiple theoretical and technological bottlenecks.

1) The development of multi-scale in situ dynamic characterization technologies is essential to monitor closed pore evolution and sodium occupancy in real-time under actual electrochemical conditions, thereby bridging the gap between idealized models and practical material performance.

2) Integrating high-throughput computing and machine learning, a full chain data-driven prediction model of "precursor structure - carbonization process - closed pore parameters - electrochemical performance" would be also constructed, which breaks through the efficiency bottleneck of traditional trial and error methods.

3) Deepen the understanding of the coupling mechanism among ion desolvation, interface SEI formation, and closed pore inlet kinetics, this achieves synergistic enhancement of ICE, rate capability, and plateau capacity. The refinement and intelligence infusion into closed pore engineering will be pivotal in advancing energy density practicalization within sodium-ion batteries.

Declaration of Competing Interest

The authors declare that they have no known competing financial interests or personal relationships that could have appeared to influence the work reported in this paper.

Acknowledgments

This work was financially supported by Fundamental Research Funds for the Universities of Henan Province (No. NSFRF240609 and NSFRF2502051), Doctoral Fund of Henan Polytechnic University (B2022-44).

References

1. N Yabuuchi, K Kubota, M Dahbi, S Komaba (2014) Research development on sodium-ion batteries. Chem Rev 114(23): 11636-11682.
2. S Nour Eddine, H Daoudi, M Kasbaji, A Chari, J Alami, et al. (2025) From biomass to energy storage: a review on lignocellulosic biomass-derived hard carbon anodes for sodium-ion batteries. Energy Fuels 39(36): 17112-17154.
3. S Jia, B Zhang, J Gao, G Jin, Y Wang, et al. (2025) Biomass-derived hard carbon anodes: from structural engineering to industrial sodium-ion battery applications. Energy Storage Mater 80: 104420.
4. T Zhao, L Yan, L Song, A Li, Y Xiong, et al. (2024) The latest research progress on closed pore hard carbon for sodium-ion batteries. J Energy Storage 102: 114209.
5. S Gan, Y Huang, N Hong, Y Zhang, B Xiong, et al. (2025) Comprehensive understanding of closed pores in hard carbon anode for high-energy sodium-ion batteries. Nano Micro Lett 17: 325.
6. W Zhang, Y Du, Y Qiu, C Li, I Razanau, et al. (2025) Closed-pore engineering in hard carbon for sodium ion storage: advances, challenges and future horizons. Adv Energy Mater 15(44): e03884.
7. Z Zheng, B Pei, L Zhang, X Cao, S Liang (2025) Pore structure in hard carbon: from recognition to regulation. Energy Storage Mater 75: 104068.
8. J Lu, Z Zhang, Y Zheng, Y Gao (2023) In situ transmission electron microscopy for sodium-ion batteries. Adv Mater 35(38): 2300359.
9. T Zheng, J N Reimers, J R Dahn (1995) Effect of turbostratic disorder in graphitic carbon hosts on the intercalation of lithium. Phys Rev B 51(2): 734-741.
10. D A Stevens, J R Dahn (2001) The mechanisms of lithium and sodium insertion in carbon materials. J Electrochem Soc 148(8): A803.
11. D A Stevens, J R Dahn (2000) Highcapacity anode materials for rechargeable sodium-ion batteries. J Electrochem Soc 147: 1271.
12. Y Cao, L Xiao, M L Sushko, W Wang, B Schwenzer, et al. (2012) Sodium Ion Insertion in Hollow Carbon Nanowires for Battery Applications. Nano Lett 12(7): 3783-3787.
13. C Bommier, T W Surta, M Dolgos, X Ji, (2015) New mechanistic insights on Na-ion storage in nongraphitizable carbon. Nano Lett 15(9): 5888-5892.
14. B Zhang, C M Ghimbeu, C Laberty, C Vix Guterl, J M Tarascon (2016) Correlation between microstructure and Na storage behavior in hard carbon. Adv Energy Mater 6(1): 1501588.
15. Y Li, Y Hu, M Titirici, L Chen, X Huang (2016) Hard carbon microtubes made from renewable cotton as high-performance anode material for sodium-ion batteries. Adv Energy Mater 6(18): 1600659.
16. H Au, H Alptekin, A C S Jensen, E Olsson, C A O Keefe, et al. (2020) A revised mechanistic model for sodium insertion in hard carbons. Energy Environ Sci 13(10): 3469-3479.
17. N Sun, J Qiu, B Xu (2022) Understanding of sodium storage mechanism in hard carbons: ongoing development under debate. Adv Energy Mater 12(7): 2200715
18. X Chen, J Tian, P Li, Y Fang, Y Fang, et al. (2022) An overall understanding of sodium storage behaviors in hard carbons by an "adsorption-intercalation/filling" hybrid mechanism. Adv Energy Mater 12(24): 2200886.
19. Z Wang, X Feng, Y Bai, H Yang, R Dong, et al. (2021) Probing the energy storage mechanism of quasi-metallic Na in hard carbon for sodium-ion batteries. Adv Energy Mater 11(11): 2003854.
20. S Alvin, D Yoon, C Chandra, H S Cahyadi, J H Park, et al. (2019) Revealing sodium ion storage mechanism in hard carbon. Carbon 145: 67-81.
21. R Li, A Hu, Z Wang, W Yang, Q He, et al. (2026) Dynamic control of crystallization rate enables efficient sodium storage in coal-based hard carbon: synergistic effects of short-range ordered structure and closed pores. J Energy Chem 112: 832-841.
22. E O Eren, E Senokos, E Scoppola, Z Song, M Antonietti, et al. (2025) An enhanced three-stage model for sodium storage in hard carbons. Energy Environ Sci 18(16): 7859-7868.
23. Y Umemoto, K Ohishi, D Igarashi, R Tatara, C Lin, et al. (2026) Multiscale insights into sodium storage in hard carbon from operando small- and wide-angle neutron scattering measurements. Chem Sci 17(15): 7466-7474.
24. D A Stevens, J R Dahn (2000) An In situ small-angle X-ray scattering study of sodium insertion into a nanoporous carbon anode material within an operating electrochemical cell. J Electrochem Soc 147: 4428.

25. L Kitsu Iglesias, E N Antonio, T D Martinez, L Zhang, Z Zhuo, et al. (2023) Revealing the sodium storage mechanisms in hard carbon pores. Adv Energy Mater 13(44): 2302171.
26. M Olsson, A Klein, N Mozhzhukhina, S Xiong, C Appel, et al. (2025) Resolving the sodiation process in hard carbon anodes with nanostructure specific X-ray imaging. Adv Sci 12(34): e08635.
27. X Chen, Y Fang, H Lu, H Li, X Feng, et al. (2021) Microstructure-dependent charge/discharge behaviors of hollow carbon spheres and its implication for sodium storage mechanism on hard carbon anodes. Small 17(34): 2102248.
28. X Liu, Z Liang, Y Xiang, M Lin, Q Li, et al. (2021) Solid-state NMR and MRI spectroscopy for Li/Na batteries: materials, interface, and in situ characterization. Adv Mater 33(50): 2005878.
29. R Alcántara, P Lavela, G F Ortiz, J L Tirado (2005) Carbon microspheres obtained from resorcinol-formaldehyde as high-capacity electrodes for sodium-ion batteries. Electrochem Solid-State Lett 8(4): A222.
30. J M Stratford, P K Allan, O Pecher, P A Chater, C P Grey (2016) Mechanistic insights into sodium storage in hard carbon anodes using local structure probes. Chem Commun 52(84): 12431-12433.
31. K Gotoh (2021) Na solid-state NMR analyses for Na-ion batteries and materials. Batter Supercaps 4(8): 1267-1278.
32. M Gabrijelčič, B Tratnik, G Kapun, E Tchernychova, N Z Logar, et al. (2025) Probing sodium structures and dynamics in hard carbon for Na-ion batteries using ^{23}Na operando solid-state NMR spectroscopy. J Mater Chem A 13(2): 1042-1056.
33. J S Weaving, A Lim, J Millichamp, T P Neville, D Ledwoch, et al. (2020) Elucidating the sodiation mechanism in hard carbon by operando raman spectroscopy. ACS Appl Energy Mater 3(8): 7474-7484.
34. Y Zhang, S W Zhang, Y Chu, J Zhang, H Xue, et al. (2025) Redefining closed pores in carbons by solvation structures for enhanced sodium storage. Nat Commun 16: 3634.
35. Y S Yun, K Y Park, B Lee, S Y Cho, Y U Park, et al. (2015) Sodium-ion storage in pyroprotein-based carbon nanoplates. Adv Mater 27(43): 6914-6921.
36. Q Xia, C L Ko, E R Cooper, Q Gu, R Knibbe, J R Harmer, et al. (2025) Elucidating sodium ion storage mechanisms in hard carbon anodes at the electronic level. Adv Funct Mater 35(28): 2421976.
37. B Sun, R Yu, Y Zhong, J Liu, Z Wei, et al. (2025) Closed pore architecture and sodium cluster deposit visualization in hard carbon. Nano Lett 25(17): 7161-7169.
38. D Saurel, B Orayech, B Xiao, D Carriazo, X Li, et al. (2018) From charge storage mechanism to performance: a roadmap toward high specific energy sodium-ion batteries through carbon anode optimization. Adv Energy Mater 8(17): 1703268.
39. T Liu, D Lu, H Shao, L Zhong, X Wu, et al. (2026) Revisiting sodium storage mechanisms in closed-pore hard carbons: nucleation vs. clustering under potential-driven charge effects. J Energy Chem 116: 933-943.
40. H Sun, Z Li, F Yuan, Z Li, Q Sun, et al. (2025) Molecular-level precursor regulation strategy: constructing hard carbon with rich closed pores for extended plateau sodium storage capacity. Chem Eng J 524: 169227.
41. Y Liu, Z Tao, L Ge, J Li, X Guo, et al. (2026) Uncovering the inherent link between pseudo-graphite structure and closed-pore formation in hard carbon. J Colloid Interface Sci 702: 138855.
42. J Lan, Q Lin, X Li, Y Cao, H Chi, et al. (2026) Tailoring the biochar microstructure to increase closed nanopores in biomass-derived hard carbons for boosting sodium-ion storage. Carbon 249: 121220.
43. Z Sun, Z Li, Y Li, Z Wang, H Zuo, et al. (2025) Unveiling a two-stage closed-pore formation mechanism in bamboo-derived hard carbons for high-plateau-capacity sodium-ion battery anodes. Chem Eng J 521: 167011.
44. H Ando, K Hashi, S Ohki, Y Hatakeyama, Y Nishina, et al. (2024) State change of Na clusters in hard carbon electrodes and increased capacity for Na-ion batteries achieved by heteroatom doping. Carbon Trends 16: 100387.
45. B Zhao, X Li, L Shang, C Qiu, R Yuan, et al. (2024) Regulating oxygen functionalities of cellulose-derived hard carbon toward superior sodium storage. J Mater Chem A 12(10): 5834-5845.
46. Y Li, D Xia, L Tao, Z Xu, D Yu, et al. (2024) Hydrothermally assisted conversion of switchgrass into hard carbon as anode materials for sodium-ion batteries. ACS Appl Mater Interfaces 16(22): 28461-28472.
47. J Xie, H Ai, K Du, R Lv (2026) Regulating ultramicropores and closed-pores in starch-derived hard carbons for efficient sodium ion storage. Carbon 247: 121077.
48. X Zhao, P Shi, H Wang, Q Meng, X Qi, et al. (2024) Unlocking plateau capacity with versatile precursor crosslinking for carbon anodes in Na-ion batteries. Energy Storage Mater 70: 103543.
49. X Liu, J Wang, B Zhang, G Zhang, K Li, et al. (2026) Programming closed pores in hard carbon: from molecular topology to chemomechanical carbonization. Energy Storage Mater 88: 105073.
50. J D Wang, T Qiu, J Xie, F Liu, J F Wu, et al. (2026) CO_2 activation-induced closed pores in hard carbon derived from bamboo for enhanced sodium-ion storage. J Colloid Interface Sci 703: 139177.
51. Z Zhang, Y Wang, K Tang, Z Chen, X Li, et al. (2025) Regulation of closed pores in hard carbon for enhanced electrochemical sodium storage. Nanoscale Horiz 10(4): 824-834.
52. Y Zhang, Y Ye, G Zhang, J Wang, K Li, et al. (2025) Oxidation anchoring strategy for the retention of nanostructures in high temperature carbonization process to enhance hard carbon sodium storage performance. Chem Eng J 503: 158395.
53. A Griffin, H Nguyen, J Aguinaga, D L Patton, Z Qiang, et al. (2026) Commodity elastomer-derived ordered mesoporous hard carbon for high-performance sodium-ion battery anodes. J Mater Chem A 14(43): 29407-29420.
54. W Hou, L Ma, A Li, H Peng, Z Liu, et al. (2024) Heteroatom doping-induced formation of closed pores for high-performance sodium storage hard carbon anodes. Chem Commun 60(62): 8055-8058.
55. Y Shen, Y Xin, Q Zhou, B Fan, Y Wang, et al. (2026) Synergistic integration of phosphorus doping and closed-pore architecture in starch-derived hard carbon for advanced sodium-ion storage. Chem Eng J 530: 173884.
56. A Yadav, S Dutta (2026) Single-atom incorporated hard carbon for atomic interface engineering of sodium-ion batteries. Mater Today Energy 57: 102230.
57. S Reiche, R Blume, X C Zhao, D Su, E Kunkes, et al. (2014) Reactivity of mesoporous carbon against water – an in-situ XPS study, Carbon 77: 175-183.
58. H Zhang, X Zhang, J Zhang, X Li, R Yuan, et al. (2026) Control of hard carbon structure via oxidative crosslinking and functional group decomposition in pitch for sodium-ion batteries. Carbon 256: 121697.
59. R Ma, Y Chen, Q Li, B Zhang, F Chen, et al. (2024) Wang, Oxygen-driven closing pore formation in coal-based hard carbon for low-voltage rapid sodium storage. Chem Eng J 493: 152389.
60. B Wang, Y Yao, W Wang, Y Xu, Y Wan, et al. (2024) Resolution of the reciprocity between radical species from precursor and closed pore formation in hard carbon for sodium storage. J Colloid Interface Sci 664: 681-690.

61. Q Hu, L Xu, G Liu, J Hu, X Ji, et al. (2024) Understanding the sodium storage behavior of closed pores/carbonyl groups in hard carbon. ACS Nano 18(32): 21491-21503.

62. Y Qiu, Y Su, X Jing, H Xiong, D Weng, et al. (2025) Rapid closed pore regulation of biomass-derived hard carbons based on flash joule heating for enhanced sodium ion storage. Adv Funct Mater 35(29): 2423559.

63. P Huang, Z Guo, Z Li, L Chen, W Liu, et al. (2025). Spatiotemporal Evolution in Hard Carbon Synthesis via Electrothermal Coupling Strategy for High-Performance Sodium-Ion Batteries. Adv Mater 37(38): 2507521.

64. J Zhu, W Feng, Q Ren, S Zhang, X Sui, et al. (2026) Synergistic engineering of closed pores and oxygenic groups via vapor-phase carbon deposition for hard carbon anodes with high initial coulombic efficiency in sodium-ion batteries. Compos Part B Eng 311: 113285.

65. K Zhang, J Teng, L Ding, X Tang, J Huang, et al. (2025) Establishing structure-property relationships grounded in oxidation strategy engineering to unravel the triggering mechanism of Na^+ filling in hard carbon closed pore. Electrochimica Acta 538: 146970.

ISSN: 2574-1241

DOI: 10.26717/BJSTR.2026.67.010421

Guiyun Yi . Biomed J Sci & Tech Res

This work is licensed under Creative *Commons* Attribution 4.0 License

Submission Link: https://biomedres.us/submit-manuscript.php

Assets of Publishing with us

- Global archiving of articles
- Immediate, unrestricted online access
- Rigorous Peer Review Process
- Authors Retain Copyrights
- Unique DOI for all articles

https://biomedres.us/